Inactivation of Yeast Phenylalanine Transfer Ribonucleic Acid by Kethoxal*

Michael Litt†

ABSTRACT: Yeast tRNA^{Phe} was labeled with tritiated kethoxal in the presence of Mg^{2+} at 25°. After 90-min reaction time, only the guanines at positions 20 and 34 were labeled to a significant extent and the RNA had lost about 50% of its phenylalanine acceptor activity. Charged and uncharged molecules of tRNA^{Phe} were separated by chromatography on benzoylated DEAE-cellulose. Both charged and uncharged molecules were derivatized at guanine sites 20 and 34. Glyoxal also reacts with tRNA^{Phe} at positions 20 and 34. However, the glyoxal derivative retains at least 90% of its phenylalanine acceptor activity. Neither site 20 nor site 34 can yet be ruled out as the target site for inactivation. It is likely that the stereoisomerism of the kethoxal adduct formed at the target site determines whether or not derivatization leads to inactivation.

Much recent work has focused on the question of how modifications in the structures of purified tRNAs affect their ability to accept amino acids. It is clear that tRNAs can be extensively modified by enzymatic degradation without loss of amino acid acceptor activity (Seno *et al.*, 1970; Schmidt *et al.*, 1970; Chuguev *et al.*, 1970). Therefore, it is of interest that the phenylalanine acceptor activity of yeast tRNA^{Phe} is partially destroyed by a reaction with kethoxal which modifies the two exposed guanine sites at positions 20 and 34 of the molecule (Litt, 1969).

In attempting to elucidate the mechanism of inactivation of tRNA^{Phe} by kethoxal, we asked which of the two sites is the target for inactivation. In this report we present the results of experiments designed to answer this question.

Methods

RNA. Unfractionated Bakers' yeast sRNA (Sigma) was used as the source for preparing tRNA^{Phe}. Two preparations were made. Preparation I, which was prepared by the method of Litt (1968), had a phenylalanine content, before deacylation, of 1800 pmoles/A_{260} unit. Preparation II was prepared by the method of D. Yoshikami (personal communication, 1970). Two-thousand A_{260} units of partially purified tRNA^{Phe} from a 4 × 90 cm BD-cellulose[1] column (Litt, 1968) was subjected to chromatography on a 1.2 × 80 cm BD-cellulose column. The column was eluted with a linear gradient (total volume 800 ml) from 0.8 to 1.8 M NaCl in 10 mM sodium acetate (pH 4.5)–1 mM EDTA. Nine-milliliter fractions were collected in tubes containing 0.2 ml of 2 M Tris-Cl–0.2 M $MgCl_2$ (pH 8.5). Fractions were assayed for tRNA^{Phe} by fluorescence (Yoshikami *et al.*, 1968). Fractions 40–80, which had a constant ratio of fluorescence intensity to A_{260}, were combined, concentrated by ethanol precipitation, redissolved in water, passed through a G-25 Sephadex column equilibrated with 0.1 mM EDTA (pH 7.0), and stored frozen at −20°. The maximum degree of charging obtained with preparation II was 1250 pmoles of phenylalanine per A_{260} unit.

Reaction of [^{3}H]Kethoxal and Glyoxal with RNA. Reaction mixtures contained, per ml of final volume, 35 A_{260} units of tRNA^{Phe}, 100 μmoles of sodium cacodylate (pH 7.0), 10 μmoles of $MgCl_2$, and 15 μmoles of ^{3}H-labeled kethoxal with a specific activity of 4 mCi/mole (Schwarz–Mann). Incubation was at 25°. Where specified, glyoxal (Matheson, Coleman & Bell) was also present. For kinetic studies, aliquots were withdrawn at intervals, mixed with 0.2 volume of 1 M sodium acetate (pH 4.5), and precipitated with 2 volumes of 95% ethanol. RNA precipitates were washed twice with 2% potassium acetate (pH 5.2) in 70% ethanol, once with 95% ethanol, and were dried *in vacuo*. After dissolution in water, samples were taken for measurement of A_{260}, acid-precipitable radioactivity (Penman *et al.*, 1964) and phenylalanine acceptor activity (Litt, 1968). Values for acceptor activity presented in this paper represent steady-state levels of charging obtained under conditions found to be optimal for unmodified tRNA^{Phe}. Kinetic studies of the aminoacylation of kethoxalated and untreated tRNA^{Phe} showed both processes had reached a steady state in less than 10 min.

Separation of Charged and Uncharged Molecules after Kethoxalation. This was accomplished by BD-cellulose chromatography of charged, phenoxyacetylated tRNA (Shulman and Chambers, 1968). We modified their method as follows. (1) $MgCl_2$ replaced $MgSO_4$ in the eluting solutions. (2) The ethanol concentration in solution III was increased to 30%. (3) After washing the columns with solution II, a linear gradient of solution II (in the mixing chamber) and solution III (in the reservoir) was used to elute the uncharged tRNA^{Phe} peak. After this peak had been eluted, the charged tRNA^{Phe} peak was stripped from the column with solution III.

Miscellaneous Methods. Radioactive samples were counted in a Packard liquid scintillation counter at 4°. Counting efficiencies were determined by internal standardization with [^{14}C]toluene or [^{3}H]water. Aqueous solutions containing salts or urea were counted in a fluor consisting of 0.3% PPO–0.03% dimethyl-POPOP dissolved in toluene–Triton X-100 (2:3, v/v) (Fox, 1968).

Digestion of tRNA with phenol-extracted T_1 RNase and

* From the Departments of Biochemistry and Medical Genetics, University of Oregon Medical School, Portland, Oregon 97201. *Received January 11, 1971.* Supported by Grant GM-16299 from the National Science Foundation and Grant CA 13173 from the National Institutes of Health.

† Career development awardee of the National Institute of General Medical Sciences.

[1] Abbreviations used are: BD-cellulose, benzoylated DEAE-cellulose; PPO, 2,5-diphenyloxazole; dimethyl-POPOP, 1,4-bis[2-(4-methyl-5-phenyloxazolyl)]benzene; 3′(2′)-GMP, 3′(2′)-guanosine monophosphate.

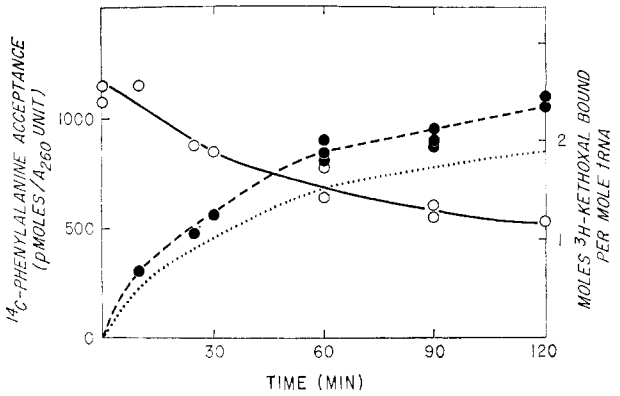

FIGURE 1: Kinetics of the reaction between [^{3}H]kethoxal with tRNA^{Phe} and of the consequent inactivation of phenylalanine acceptance. Closed circles and dashed curve, [^{3}H]kethoxal bound to tRNA^{Phe}; dotted curve, [^{3}H]kethoxal remaining bound to tRNA^{Phe} after assay for phenylalanine acceptance; open circles, phenylalanine acceptance.

chromatography on DEAE-cellulose columns were performed as previously described (Litt, 1969) except that all eluents contained 20 mM Tris–20 mM boric acid adjusted to pH 7.5 with HCl instead of 20 mM Tris adjusted to pH 8.0 with boric acid.

The kinetics of reactions between kethoxal or glyoxal and 3′(2′)-GMP were measured as previously described (Litt and Hancock, 1967) except that a Gilford spectrophotometer, equipped with a thermostatted cell compartment was used and the solvent for the reaction was 0.1 M sodium cacodylate–0.01 M $MgCl_2$ (pH 7.0). The rates of decomposition of the glyoxal and kethoxal adducts of 3′(2′)-GMP were measured as follows. The adducts were prepared by overnight incubation at 25° of reaction mixtures containing 11 mM GMP, 520 mM glyoxal, or 23 mM kethoxal in 0.1 M sodium cacodylate–0.01 M $MgCl_2$ (pH 7.0). These reaction mixtures were diluted 100-fold into 0.1 M Tris-chloride (pH 7.6) and their absorbances at 270 nm were followed at 25°.

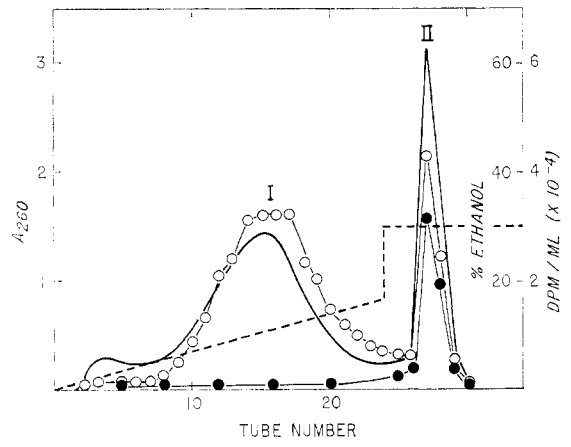

FIGURE 2: Separation of charged and uncharged tRNA^{Phe} molecules after reaction with [^{3}H]kethoxal. Phenoxyacetylated, charged, kethoxalated tRNA^{Phe} (52 A_{260} units) was chromatographed on a 0.4 × 11 cm column of BD-cellulose. Fractions (2.5 ml) were collected at a flow rate of 15 ml/hr. Solid line, A_{260}; open circles, [^{3}H]kethoxal; closed circles, [^{14}C]phenylalanine; dashed line, per cent ethanol in the eluting solution. The early region of the elution profile, corresponding to the wash with solution II, did not exhibit significant amounts of tRNA or radioactivity and hence is not shown here.

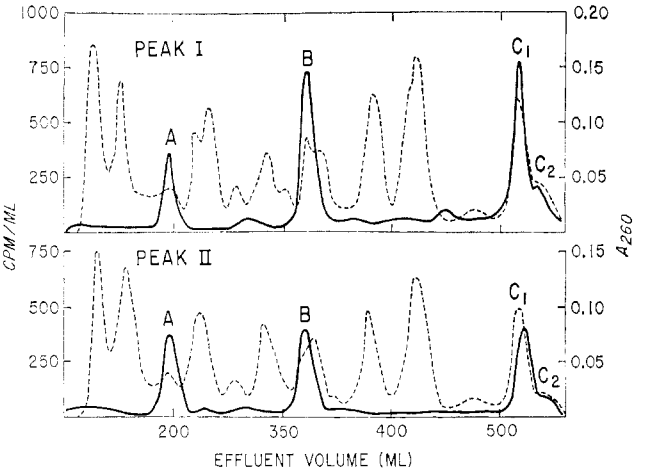

FIGURE 3: Elution profiles of T_1 RNase digests of tRNA^{Phe} from peak I (uncharged molecules) and peak II (charged molecules) of Figure 2. Digests (14 A_{260} units) were applied to 0.4 × 120 cm columns of DEAE-cellulose. Columns were eluted with linear gradients (total volume 800 ml) from 0 to 0.4 M NaCl in 0.02 M Tris-borate-chloride (pH 7.5)–7 M urea. Flow rates were 12–16 ml/hr. Solid line, radioactivity of ^{3}H from the [^{3}H]kethoxal used; dashed line, A_{260}.

Results

Inactivation of tRNA^{Phe} by Kethoxal. Figure 1 shows the time course of binding of [^{3}H]kethoxal and inactivation of tRNA^{Phe} at 25°. After 90 min, about two moles of kethoxal have been bound and the extent of phenylalanine acceptance has decreased to about 50% of the level shown by the starting material. Both kethoxal binding and loss of phenylalanine acceptance are reversed to the extent of 90–95% by overnight incubation of the kethoxalated tRNA^{Phe} in 0.1 M Tris-Cl$^-$ (pH 7.6) at 37°. About 20% of the [^{3}H]kethoxal is removed from the tRNA during the 15-min incubation at pH 7.6 and 25° used for assay of phenylalanine acceptance.

Separation of Charged and Uncharged Molecules. tRNA^{Phe} labeled with [^{3}H]kethoxal for 90 min was charged with [^{14}C]-phenylalanine (4 mCi/mmole), phenoxyacetylated, and chromatographed on BD-cellulose (Figure 2). ^{3}H-Labeled uncharged molecules (peak I) were eluted well ahead of ^{3}H- and ^{14}C-labeled charged molecules (peak II). The ^{3}H specific activity of peak II was about 75% of that of peak I. Peak I is heterogeneous with respect to degree of kethoxalation, with more highly kethoxalated molecules eluting later. Peak II had a phenylalanine content of 1770 pmoles/A_{260} unit.

Fingerprinting of Charged and Uncharged Molecules. Peaks I and II from the BD-cellulose column (Figure 2) were digested with T_1 RNase and chromatographed on DEAE-cellulose columns (Figure 3). The radioactive peaks B and $C_1 + C_2$ have been previously shown to contain fragments containing kethoxal at positions 20 and 34 of the tRNA^{Phe} chain (Litt, 1969). Radioactive peak A was not seen in prior work.

The relative yields of radioactivity recovered in peaks A, B, and $C_1 + C_2$ in three experiments with two different preparations of tRNA^{Phe} are shown in Table I. It is clear that peak B and peak $C_1 + C_2$ are present in fingerprints of both uncharged and charged molecules. The ratio of radioactivity in peak $C_1 + C_2$ to radioactivity in peak B has a similar value for both charged and uncharged molecules.

When T_1 RNase digests of charged or uncharged molecules were chromatographed immediately after digestion, peak A was absent (expt 3, Table I). If, however, the digests were

TABLE I: Recovery of [^{3}H]Kethoxal in Peaks A, B, and $C_1 + C_2$ from Fingerprints of T_1 RNase Digests of Charged and Uncharged Molecules.

	% of ^{3}H cpm Recovered in Peak			
	A	B	$C_1 + C_2$	$(C_1 + C_2^a)$/ B
Expt 1[b]				
Uncharged molecules	17	25	35	1.4
Charged molecules	29	15	21	1.3
Expt 2[c]				
Uncharged molecules	9	22	32	1.4
Charged molecules	23	27	34	1.2
Expt 3[b,d]				
Uncharged molecules	<0.3	32	40	1.2
Charged molecules	2	29	29	1.0

[a] This is the ratio of ^{3}H counts per minute in peaks $C_1 + C_2$ to ^{3}H counts per minute in peak B. [b] tRNA^{Phe} preparation I was used. [c] tRNA^{Phe} preparation II was used. [d] In expt 3, T_1 RNase digests were chromatographed immediately after digestion.

TABLE II: Effect of Glyoxal on Incorporation of [^{3}H]Kethoxal into and Inactivation of Phenylalanine tRNA.[a]

Molarity of Glyoxal	[^{3}H]Kethoxal Inc[b]	Phe Acceptance[c]
0	2.24	44
0.33	1.08	60
0.83	0.73	60
1.66	0.46	74

[a] Glyoxal, at the concentrations indicated, was added to standard reaction mixtures for kethoxalation of tRNA^{Phe} and the mixtures were incubated for 2 hr at 25°. [b] Moles of [^{3}H]kethoxal per mole of tRNA^{Phe}. [c] Per cent of acceptance of a control preparation incubated as above but with kethoxal and glyoxal omitted.

stored frozen at −20° before chromatography, peak A was present. The proportion of radioactivity recovered as peak A increased with increased storage time. We conclude that peak A is probably derived from kethoxal which has been removed from the ologonucleotides during storage of the T_1 RNase digests.

Rates of Reaction of Glyoxal and Kethoxal with 3′(2′)-GMP. The pseudo-first-order reactions of kethoxal and glyoxal, each at a concentration of 14 mM, with 3′(2′)-GMP were followed at pH 7.0 and 27°. The half-times of the reactions were 1.7 min for kethoxal and 55 min for glyoxal. The decomposition rates of the kethoxal and glyoxal adducts of 3′(2′)-GMP were measured in 0.1 M Tris-chloride (pH 7.6) at 25°, the same pH and temperature used for phenylalanine acceptor assays. Under these conditions the kethoxal adduct had a half-life of 2 hr, and the glyoxal adduct had a half-life of approximately 20 hr.

Effect of Glyoxal on Incorporation of [^{3}H]Kethoxal into tRNA^{Phe} and on Inactivation of tRNA^{Phe}. When nonradioactive glyoxal was added to the mixtures for reaction of [^{3}H]kethoxal with tRNA^{Phe}, it decreased both the extent of incorporation of [^{3}H]kethoxal into the RNA and the extent of inactivation of phenylalanine acceptor ability (Table II). Addition of 0.64 M glyoxal to the standard kethoxalation mixture reduced the extent of kethoxalation at 90 min by 70%. When tRNA^{Phe} was incubated for 90 min with 0.64 M glyoxal, but *without* kethoxal, 90% of the phenylalanine acceptor activity was retained.

Discussion

We have observed that kethoxalation of tRNA^{Phe} to the extent of approximately 2 moles/mole of tRNA causes a 50–60% drop in phenylalanine acceptance. The major sites of attachment of the kethoxal are at guanine-20 in the dihydrouridine loop and at guanine-34 in the anticodon loop.

By separating charged from uncharged molecules after kethoxalation and aminoacylation, we had hoped to identify which of the two sites was the target for inactivation. However, it is clear from Figure 3 that both charged and uncharged peaks contain molecules which have reacted with kethoxal at positions 20 and 34.

A theory which explains these results is that tRNA^{Phe} molecules remain active unless both sites 20 and 34 have been kethoxalated. Hence the ^{3}H-labeled molecules in peak II (Figure 2) would be a mixture of molecules kethoxalated only at site 20 and molecules kethoxalated only at site 34. This theory does not explain the fact that derivatization of tRNA^{Phe} with glyoxal fails to inactivate the acceptor activity, even though such derivatization protects tRNA^{Phe} against reaction with and inactivation by kethoxal.

The structure of the reaction products of guanine with glyoxal (Ia) and kethoxal (1b), as determined by Shapiro *et al.* (1969), are shown below.

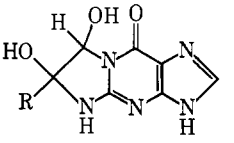

Ia, R = H
Ib, R = $CH_3CH(OC_2H_5)$

It is clear that Ia and Ib can each exist in four optically isomeric forms. To account for our results, we propose that kethoxal can react with the target G site to produce several (perhaps all) of these forms. Some of the isomers formed remain active in phenylalanine acceptance, whereas others are inactive.

This hypothesis is supported by the results obtained when glyoxal, or a glyoxal–kethoxal mixture, reacts with tRNA^{Phe}. As radioactive glyoxal is not readily available, we could not easily determine the extent or the specificity of the reaction of glyoxal with tRNA^{Phe}. However, we were able to show (Table II) that nonradioactive glyoxal inhibited the reaction of radioactive kethoxal with tRNA^{Phe}. That the inhibition follows a pattern which would be predicted if glyoxal and kethoxal were competing for the same sites can be seen from the following considerations.

Let k_{GI} and k_K represent the second order rate constants for reaction of glyoxal and kethoxal with exposed guanine sites in tRNA^{Phe}. Let [GI] and [K] represent the number of guanine

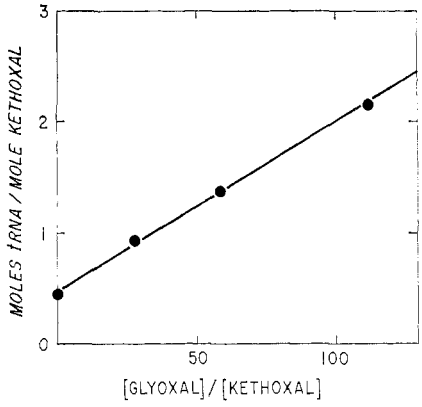

FIGURE 4: Effect of nonradioactive glyoxal on the reaction of $tRNA^{Phe}$ with [^{3}H]kethoxal.

sites per tRNA molecule which have reacted with glyoxal and kethoxal, respectively. Since both glyoxal and kethoxal are in great excess during the reactions, the reactions will follow pseudo-first-order kinetics and the molar ratio of the glyoxal and kethoxal derivatives formed will be given by eq 1 (Frost and Pearson, 1961).

$$\frac{[Gl]}{[K]} = \frac{k_{Gl}[\text{glyoxal}]}{k_K[\text{kethoxal}]} \quad (1)$$

Assume further that there are a definite number, N, of exposed guanine sites, all of which react with either kethoxal or glyoxal during the 2-hr reaction at 25°. Hence, [Gl] + [K] = N. Substituting this in eq 1, we find

$$\frac{1}{[K]} = \frac{1}{N} + \frac{1}{N}\frac{k_{Gl}[\text{glyoxal}]}{k_K[\text{kethoxal}]} \quad (2)$$

Hence, a plot of the reciprocal of the extent of kethoxalation *vs* the [glyoxal]/[kethoxal] ratio should be linear with a slope/intercept ratio k_{Gl}/k_K. The data of Table II are plotted in this way in Figure 4. A straight line is observed with a slope/intercept ratio of 0.111. This compares to a ratio k_{Gl}/k_K of 0.031 derived from direct measurement of the rates of kethoxalation and glyoxalation of 3′(2′)-GMP. We speculate that the difference between these values is attributable in the former case to the incorporation of G into a macromolecule. This would be expected to hinder the reaction of kethoxal with G sites to a greater extent than it would hinder the reaction of glyoxal, a smaller and more symmetrical reagent.

Under certain conditions, glyoxal, but not kethoxal, can react with cytosine and adenine sites in RNA (Shapiro *et al.*, 1970). Since we used nonradioactive glyoxal, such modifications would not have been detected in our work. If they did occur, they had no effect on phenylalanine acceptance by $tRNA^{Phe}$.

At first sight, the mechanism which we have proposed for inactivation of $tRNA^{Phe}$ by kethoxal does not seem to be consistent with our observation that uncharged molecules contain more kethoxal than the average whereas charged molecules contain less. However, since about 20% of the kethoxal is removed from the tRNA during aminoacylation, there will be a certain degree of reactivation during this process. Some of the reactivated molecules will be aminoacylated and will therefore dilute the kethoxal content of the charged molecules.

Dudock *et al.* (1970) have shown that purified yeast phenylalanyl-tRNA synthetase can aminoacylate *Escherichia coli* $tRNA_1^{Val}$ as well as yeast and wheat germ $tRNA^{Phe}$. As the dihydrouridine loop and stem are exceedingly similar in all three of these molecules, these workers suggest that this region is part of the synthetase recognition site. The work of Seno *et al.* (1970) with *E. coli* formylmethionine tRNA suggests that the stem of the dihydrouridine loop, and not the major portion of the loop itself, is essential for amino acid acceptance by tRNA. Although we cannot yet rule out position 34 as the target site for inactivation of $tRNA^{Phe}$ by kethoxal, the aforementioned results make it probable that the target site is at position 20 in the dihydrouridine loop.

This proposal is consistent with the data of Seno *et al.* (1970) because inactivation by kethoxal seems to be due to steric hindrance by an appropriately oriented group preventing the synthetase from attaining sufficiently close contact with the tRNA. Removal of part of the dihydrouridine loop, as accomplished by Seno *et al.* (1970), would not be expected to cause such steric hindrance. It is also of interest to point out that residues 21 and 22 in the dihydrouridine loop of formylmethionine tRNA were not removed by Seno *et al.* Residue 21 in formylmethionine tRNA is homologous to residue 20 in $tRNA^{Phe}$, the presumed target for inactivation by kethoxal.

By studying the kethoxalation of $tRNA^{Phe}$ while it is complexed to other appropriate macromolecules, such as polyuridylic acid and 30S ribosomal subunits or phenylalanyl-tRNA synthetase, we hope to remove the ambiguity in the present report and to identify precisely the target site for inactivation.

Acknowledgments

I am indebted to Joann van Dolah and Carrol Platz for expert technical assistance.

Added in Proof

We have recently found that partial kethoxalation of *E. coli* $tRNA_1^{Val}$, performed as described for yeast $tRNA^{Phe}$ in this paper, has no effect on the chargeability of the $tRNA_1^{Val}$ as assayed with [^{14}C]valine and crude *E. coli* synthetases. Such kethoxalation does cause approximately 50% loss in chargeability of $tRNA_1^{Val}$ as assayed with [^{14}C]phenylalanine and crude yeast synthetases. As *E. coli* $tRNA_1^{Val}$ contains no G's in its anticodon but does have a G at position 20, these observations strongly support the notion that position 20 is the target site for inactivation of yeast $tRNA^{Phe}$ by kethoxal.

References

Chuguev, I. I., Axelrod, V. D., and Baev, A. A. (1970), *Biochem. Biophys. Res. Commun. 41*, 108.

Dudock, B. S., DiPeri, C., and Michael, M. S. (1970), *J. Biol. Chem. 245*, 2465.

Fox, B. W. (1968), *Int. J. Appl. Radiat. Isotopes 19*, 717.

Frost, A. A., and Pearson, R. G. (1961), Kinetics and Mechanism, 2nd ed, New York, N. Y., Wiley, pp 160–162.

Litt, M. (1968), *Biochem. Biophys. Res. Commun. 32*, 507.

Litt, M. (1969), *Biochemistry 8*, 3249.

Litt, M., and Hancock, V. (1967), *Biochemistry 6*, 1848.

Penman, S., Becker, Y., and Darnell, J. E. (1964), *J. Mol. Biol. 8*, 541.

Schmidt, J., Buchardt, B., and Reid, B. R. (1970), *J. Biol. Chem. 245*, 5743.
Seno, T., Kobayashi, I., Fukuhara, M., and Nishimura, S. (1970), *FEBS (Fed. Eur. Biochem. Soc.) Lett. 7*, 343.
Shapiro, R., Cohen, B. I., and Clagett, D. C. (1970), *J. Biol. Chem. 245*, 2633.
Shapiro, R., Cohen, B. I., Shivey, S., and Maurer, H. (1969), *Biochemistry 8*, 238.
Shulman, L. H., and Chambers, R. W. (1968), *Proc. Nat. Acad. Sci. U. S. 61*, 308.
Yoshikami, D., Katz, G., Keller, E. B., and Dudock, B. S. (1968), *Biochim. Biophys. Acta 166*, 714.

A Physical Study of the Stability of the Native Nucleohistone Conformation to Salt Dissociation and Heating*

R. A. Garrett†

ABSTRACT: The subjection of nucleohistone to both salt dissociation and heating results in a loss of supercoiled structure over the salt range 0.9–1.1 M NaCl and the temperature range 64–80°. The loss of structure commences when about 60% of the histones are dissociated by salt, and approximately at the temperature at which the DNA in nucleohistone melts. The conformation of F1-histone-deficient-soluble nucleohistone was lost in approximately the same temperature range. No concurrent conformational change was detected in the B-DNA after either salt dissociating the histones, or heating and cooling the nucleohistone, but in both circumstances conformational changes were detected in the histones.

X-Ray diffraction investigations on isolated nucleohistone now provide very strong evidence for the presence of a native supercoiled conformation of individual nucleohistone molecules. The evidence rests on the interpretation of a simple partially oriented X-ray diffraction pattern with semimeridionally oriented reflections at 110, 55, 37, 27, 22, and 18 Å, where the 110-Å reflection is assumed to derive from the pitch of the superhelix and the other reflections are secondary maxima (Wilkins *et al.*, 1959; Pardon, 1966; Pardon *et al.*, 1967; Pardon, 1967; J. Pardon and M. H. F. Wilkins, manuscript in preparation). While this evidence is strong in itself, it is not conclusive. However, supporting evidence for this structure is available. First, X-ray diffraction patterns from whole nuclei show the same secondary maxima as those from extracted nucleohistone (Wilkins, 1956). Second, electron microscope investigations on chromatin reveal hollow tubular structures which are compatible with supercoiled nucleohistone of the above dimensions (Davies, 1968; Davies and Small, 1968). Third, a sedimentation study of F1-deficient-soluble nucleohistone at increasing stages of salt dissociation indicated a large conformational change compatible with the loss of supercoiled conformation (Garrett, 1970).

The main purpose of this work was to follow in detail the loss of conformation with salt dissociation and heat melting of the complex using the characteristic X-ray pattern as a criterion for the presence of the native conformation (Richards *et al.*, 1970).

The chemistry of the dissociation of histones by salt has been thoroughly investigated (Ohlenbusch *et al.*, 1967), and was further characterized by optical rotatory dispersion measurements. The heat melting of soluble nucleohistone was characterized by measuring hyperchromicity and sedimentation coefficient changes.

Materials and Methods

Preparation of Soluble Nucleohistone. The modified standard procedure was used (Zubay and Doty, 1959; Garrett, 1970). The source of nucleohistone was calf thymus. This was frozen in Dry Ice within 30 min of the calf's death. It was stored in Dry Ice and used within 3 months of collection. Observations were made on several preparations over a period of 1 year. The final concentration of nucleohistone was approximately 0.4 mg/ml in 0.7 mM sodium phosphate buffer at pH 6.8. F1-histone-deficient-soluble nucleohistone was prepared as previously described (Garrett, 1970). Both soluble nucleohistone, and F1-histone-deficient nucleohistone, preparations were invariably characterized by their respective sedimentation coefficients of 26 (±3) S and 55 (±5) S; in the extraction buffer, and by their capacity, in fibers to yield the characteristic nucleohistone low-angle X-ray pattern (Figure 1A). The properties of these nucleohistones have been described elsewhere (Garrett, 1970, 1971).

Salt-Dissociation Experiments. Gradual loss of histones from the nucleohistone complex was achieved by increasing the salt concentration of F1-deficient nucleohistone solutions.

Increments of 2.6 M NaCl–0.1 M sodium phosphate buffer (pH 6.8) were added with rapid stirring to 25-ml aliquots of the 0.6 M NaCl extract. Solutions were adjusted to 0.7, 0.8, 0.9, 1.0, 1.1, 1.2, 1.3, 1.4, 1.5, 1.6, and 1.8 M NaCl so as to cover completely the histone dissociation salt range (Ohlenbusch *et al.*, 1967). The partially dissociated nucleohistone was pelleted in 12 hr at 40,000 rpm in a Spinco "40" rotor. Solutions were investigated for optical rotatory dispersion differences. Fibers of the gels were examined by X-ray diffraction.

Heating Experiments. Aliquots (25 ml) of nucleohistone

* From the M. R. C. Biophysics Research Unit, London W. C. 2, U. K., and Max-Planck-Institut für Molekulare Genetik, Berlin-Dahlem, West Germany. *Received December 4, 1970.*

† Present address: Max-Planck-Institut für Molekulare Genetik, 1 Berlin 33, West Germany.